

Measurement of Fat/Water Ratios in Rat Liver Using 3D Three-Point Dixon MRI

Xiaowei Zhang,¹ Mark Tengowski,² Lisa Fasulo,² Suzanne Botts,² Steve A. Suddarth,¹ and G. Allan Johnson^{1*}

Hepatic steatosis, or fatty liver, is commonly observed during the animal phase of drug safety studies. A noninvasive three-dimensional (3D) three-point Dixon method was used to quantitatively evaluate the fatty livers of rats induced by an experimental microsomal transfer protein (MTP) inhibitor, in an effort to develop a safety biomarker that could be translated to human studies. The method was implemented at 2.0 T for in vivo studies, and at 7.1 T for higher-resolution magnetic resonance (MR) histologic studies. In three separate protocols to study dose response and longitudinal evolution, intrahepatic fatty accumulation was detected by this method and confirmed by chemical and histologic assessments. Consistent with the pathologic changes, the fat/water ratios estimated by the MR technique increased significantly at doses of 1 mg/kg and 100 mg/kg of MTP inhibitor after 14 days of continuous administration. Among the more important findings were: 1) with the 3D three-point Dixon method, in vivo longitudinal studies of liver fat distribution can be conducted at significantly higher resolution than has previously been reported; 2) MR histology allows delineation of distribution at the microscopic scale of 0.0024 mm³ resolution; and 3) the 3D three-point Dixon technique provides relative estimates of liver fat content and distribution at a high confidence level. This technique will be applicable in future studies in which fatty liver is a potential safety issue. Magn Reson Med 51:697–702, 2004. © 2004 Wiley-Liss, Inc.

Key words: fatty liver; three-point Dixon method; fat/water ratio; volume image; resolution

A common finding in drug safety studies is fatty liver, which is the result of diet, stress, or compounds that modify lipid metabolism in the liver. The development of noninvasive methods to detect the onset and progression of, and recovery from fatty liver would be a valuable aid for the early determination of compound toxicity.

The use of decomposing fat and water signals to discriminate between fat and water protons based on their resonant frequency difference was first introduced by Dixon (1). This method uses two acquisitions with a delay between the radiofrequency (RF) and gradient echoes, such that the phase shift between water and fat is either 0 or π radians (in-phase and out-of-phase, respectively). Separate

water and fat images can be obtained by adding and subtracting the in-phase and out-of-phase images. This method was subsequently enhanced to accommodate magnetic field (B_0) and RF inhomogeneity through the use of a third acquisition, leading to the three-point Dixon method (2,3).

The microsomal transfer protein (MTP) inhibitor family of drugs has subnanomolar potency in the inhibition of lipid transfer and apolipoprotein B secretion of hepatocytes. Thus, MTP inhibitors have a potential application as therapeutic agents to lower atherogenic lipoprotein in humans. MTP inhibitor studies (both experimental and clinical) (4–6) have provided visual and biochemical evidence of hepatocellular triglyceride (TG) accumulation. Quantification of the TG-filled droplets within the hepatocytes is of interest in the evaluation of MTP inhibitors under metabolic and hepatotoxic conditions. A definitive determination of the hepatic fat fraction generally requires percutaneous biopsy, but even this invasive technique is sometimes compromised by sampling errors. The increase in liver TG content induced by MTP inhibitors is reversible, and therefore is amenable to experimental manipulation. Previous reports indicated that a plateau of fat deposition in the liver after 1 week of treatment returned to control levels 48 hr after the termination of the treatment regimen (4). Thus, the use of MTP inhibitors should be an excellent model for modulation of fat in the rat liver during a longitudinal study.

In this study we tested the 3D three-point Dixon method to determine its strengths and weaknesses as a noninvasive means of following changes in fat deposition in the liver, using the well-characterized MTP inhibitors. The main challenge in performing studies in the rat is obtaining sufficient volume resolution. A laboratory rat, at approximately 200 g, is about 500 times smaller than a human. A typical voxel in a clinical study is $1 \times 1 \times 10$ mm (10 mm³). To derive meaningful inferences about the distribution of any fat deposition in the rat liver, one should scale the voxels in human studies by roughly 500 to obtain voxel volumes of 0.02 mm³. Such gains in spatial resolution are not easily achieved. To achieve higher spatial resolution, we implemented the 3D three-point Dixon method using 3D spin warp encoding at a spatial resolution of 0.089 mm³ in vivo, and 0.0024 mm³ for ex vivo fixed specimens.

MATERIALS AND METHODS

Animal Study Groups

Dose Response Study

Fifteen CD female rats (4 weeks old, body weight = 180–210 g; Charles River, Wilmington, MA) were included in

¹Center for In Vivo Microscopy, Duke University Medical Center, Durham, North Carolina.

²Pfizer Global Research and Development, Groton Laboratories, Drug Safety Evaluation, Groton, Connecticut.

Grant sponsor: NCI; Grant numbers: 1 R24 CA92656; Grant sponsor: Pfizer, Inc.

*Correspondence to: G. Allan Johnson, Center for In Vivo Microscopy, Duke University Medical Center, Box 3302, Durham, NC 27710. E-mail: gaj@orion.duhs.duke.edu

Received 31 March 2003; revised 18 September 2003; accepted 21 October 2003.

DOI 10.1002/mrm.20005

Published online in Wiley InterScience (www.interscience.wiley.com).

© 2004 Wiley-Liss, Inc.

this study. These rats were individually housed and freely fed a regular diet and water ad libitum. The room in which the animals were kept was maintained at 20°C and 20% humidity for 1 week before (acclimation) and during (in-life) the experiment. The rats were randomly divided by weight into three dose groups, with five rats per group: 1) 0 dose (vehicle control), 2) 1 mg/kg of MTP inhibitor, and 3) 100 mg/kg of MTP inhibitor. The MTP inhibitor was freshly prepared with 25 mMol citrate buffer (pH 3). The dose was administered daily by oral gavage for 14 days under a brief period of anesthesia using isoflurane (IsoFlo; Abbott Laboratories, North Chicago, IL). The vehicle control animals were treated with an equal volume of citrate buffer only. During in-life treatment, animals were given free access to rodent chow and water.

Longitudinal Imaging Study

Twelve CD female rats of the same strain and body weight as those in the dose study were divided into two groups, with six rats in each group: 1) 1 mg/kg oral daily dose, and 2) citrate buffer control. The animals were imaged longitudinally before treatment and after 1, 4, 7, 10, and 14 days of treatment.

Ex Vivo Liver Specimen Study

Thirty rats of the same strain and body weight as those in the dose study were orally dosed with compound at 1 mg/kg and killed in a staggered fashion after 1, 4, 7, 10, and 14 days of treatment. Five animals treated with buffer only were used as a vehicle control. The liver specimens were maintained in 10% buffered formalin. The left lobe of the liver was cut into a cylinder (diameter = $8 \times 10 \text{ mm}^2$) and placed into the barrel of a 3-ml syringe filled with proton-free perfluoro-polyether Fomblin (Ausimont USA, Thorofare, NJ) for imaging at 7.1 T.

3D Three-Point Dixon Data Acquisition

The three-point Dixon method described by Glover and Schneider (3) was implemented with an additional phase-encoding lobe along the slice-selection axis (7). The resulting sequence produced three registered volumes with the refocusing pulse time shifted to produce phase differences of 0, π , and $-\pi$ radians. We incorporated the efforts of previous investigators to remove additional sources of error. Field mapping was used to remove B_0 inhomogeneity (2,3), and careful spectroscopic measurement of τ limited errors due to inaccuracies in the phase calculation (16). The chemical shift frequency change (δ) was approximately 273 Hz at 2 T, and 1041 Hz at 7.1 T. The relative phase shift (in radians, $\Delta\phi$) of liver lipid is $2\pi\delta$. The shift (in μs) required to displace the 180° RF pulse by $\pi/2$ is $\tau = \pi/(2\Delta\omega)$, i.e., 916 and 240 μs for 2 T and 7.1 T, respectively.

Live Animal Studies

The rats were weighed and then given an initial intraperitoneal injection of methohexital (45 mg/kg; Brevital; Eli Lilly, Indianapolis, IN) and atropine sulfate (0.35 mg/kg) prior to endotracheal intubation. ECG electrodes were se-

cured to the footpads with tape and a thermistor was placed in the rectum to remotely monitor body temperature. The rats were ventilated mechanically using a ventilator designed explicitly for in vivo MR microscopy (8). A stable plane of anesthesia was obtained using isoflurane at a vaporizer setting adjusted to 1–3%, depending on individual needs. Vital signs were then monitored continuously and the anesthesia was adjusted to maintain the heart rate at a normal level (300–375/min) (8). The body temperature was maintained at 37°C by circulating warm air through the bore of the magnet. Each rat was restrained in the prone position by an acrylic stage and tape. The rat was then situated in a 6-cm-diameter, custom-constructed birdcage RF coil (9). Standards consisting of three 5-mm quartz tubes containing 70% and 30% mineral oil, emulsified with a vibrator and distilled water, were placed on the animal within the imaging field. MRI was performed on a 2 T, 30-cm bore magnet controlled by a GE Medical System Signa console (Epic version 5.2). The pulse sequence parameters were: TR/TE = 700/5.4 ms, FOV = $50 \times 50 \times 18.8 \text{ mm}$, and matrix = $256 \times 128 \times 16$, resulting in voxels of $0.20 \times 0.39 \times 1.18 \text{ mm}^3$ and a total scan time of 23.8 min. The TR was chosen to accommodate scan synchronous ventilation with a respiratory rate of 80 breaths/min (8).

Ex Vivo Liver Specimen Study

A study of fixed liver specimens was performed at 7.1 T to determine the spatial heterogeneity of TG deposition at microscopic resolution. The system was controlled by a GE Medical Systems Signa console (Epic version 5.2; identical to that used on the 2 T magnet). Specimens were scanned in a 1-cm-diameter, single-sheet solenoid coil. The same 3D three-point Dixon technique was used. The shift required for the refocusing RF pulse was 240 μs , as established spectroscopically. Other pulse sequence parameters were: TR/TE = 500/9 ms, FOV = $16 \times 16 \times 10 \text{ mm}$, matrix = $256 \times 256 \times 16$, and total imaging time = 34.1 min, yielding a spatial resolution of $0.0625 \times 0.0625 \times 0.625 \text{ mm}^3$.

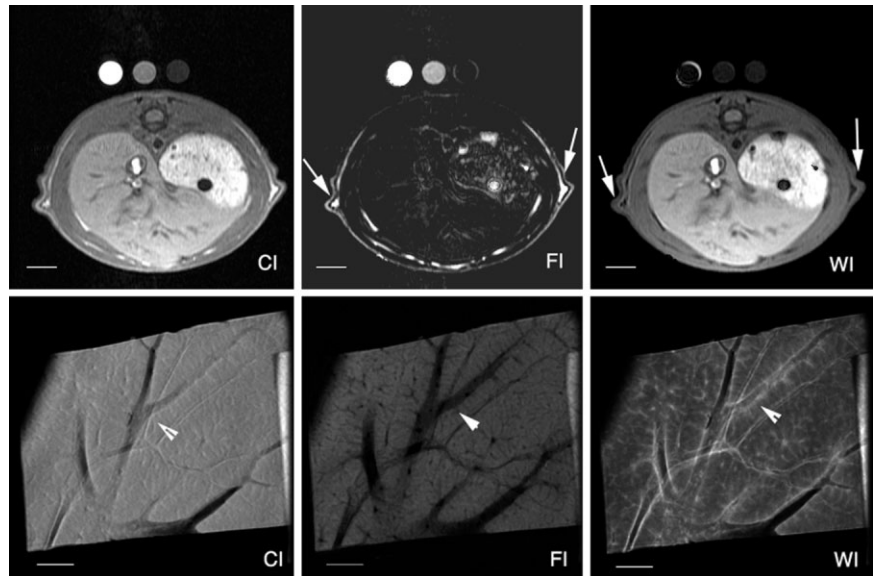
Data Processing

The three resulting volume image sets were processed on a slice-by-slice basis using the methods outlined by Glover and Schneider (3) to yield three calculated volume arrays: 1) the sum of the magnitude of the fat and water components, 2) the magnitude of the fat component, and 3) the magnitude of the water component.

Histologic and Triglyceride Level Analyses of the Livers

The animals were killed by intraperitoneal pentobarbital overdose followed by exsanguination immediately after the final imaging time point. The livers were removed and weighed. Two cross sections of liver were excised from the center and left lobes, immersed in 10% buffered formalin, and processed for both oil red O and hematoxylin and eosin (H&E) staining. The remaining liver was plunge-frozen in liquid nitrogen, maintained at -20°C , and prepared for quantitative measurement of triglyceride levels

FIG. 1. Comparison of the representative images from the in vivo study at 2 T and the specimen study at 7.1 T. Note that the subcutaneous fat and 70% and 30% of mineral oil phantoms (left and middle tubes) are clearly seen on the fat image and are suppressed on the water image (arrows). Branches of the portal venae are clearly seen on the coronal view of the specimens (arrowheads), and the lobulation of the liver is now evident. (CI = composite fat + water image; FI, fat image; WI, water image; top row, in vivo studies; bottom row, specimen images; bars: 5 mm for in vivo, and 2 mm for specimen).



using a chloroform extraction technique. The triglyceride levels were calculated as mg/g of liver tissues.

Analysis of Liver Images

The signal intensity in the images was acquired with operator-defined regions of interest (ROIs) at the same location in both fat and water images using Image J (<http://rsb.info.nih.gov/ij/>). To minimize the impact of aliasing artifacts along the slice-encoding axis in live animal studies, the analysis was centered on six slices in the center of the slice-encoding axis (slices >5 and <11). A total of 24 ROIs per animal (10 × 10 pixels per ROI, and four ROIs per slice) were acquired, with care given to placement of the ROIs to avoid confounding anatomy (e.g., large blood vessels). Fat/water ratios were calculated on a pixel-by-pixel basis by dividing the calculated fat image by the water image. For the specimen images, each specimen was measured with eight ROIs (10 × 10 pixels per ROI, four ROIs per slice, and two slices per specimen).

Statistical Methods

The data are summarized by sample mean ± SD. The differences in the fat/water ratio before and after induction of fatty livers, and between dosed and vehicle control animals were analyzed with one-tailed, paired-sample *t*-tests.

RESULTS

The integration of scan synchronous ventilation and 3D encoding allowed us to effectively suppress ventilatory motion and routinely obtain thin (1.18 mm) slices with excellent signal-to-noise ratio (SNR). Respiratory motion has a particularly confounding effect in the liver, where motion along the longitudinal axis is easily in excess of 5–8 mm over a single ventilatory cycle. The serial images acquired on all groups of animals showed a constant and satisfactory quality, as seen with the representative images

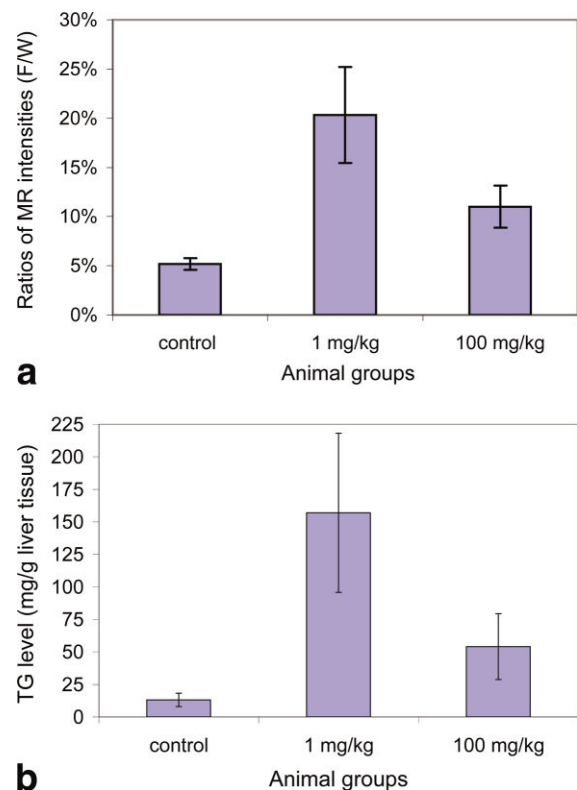


FIG. 2. The means of the (a) fat/water image ratios and (b) TG levels in three dose-group animals. The 1-mg/kg dose-treated animals were markedly increased to 20% ± 5% compared to the control animals (5% ± 0.6%; $P < 0.01$). The 100-mg/kg dose-treated animals ($N = 5$) showed a lower fat content than the 1-mg/kg dose group ($N = 5$), but a higher one than the control animals ($N = 5$; $P < 0.01$). The MRI fat/water ratio measurements were correlated with the quantitative measurement of triglyceride levels in the livers. The data represent the mean values ± SD averaged from 10 animals. [Color figure can be viewed in the online issue, which is available at www.interscience.wiley.com.]

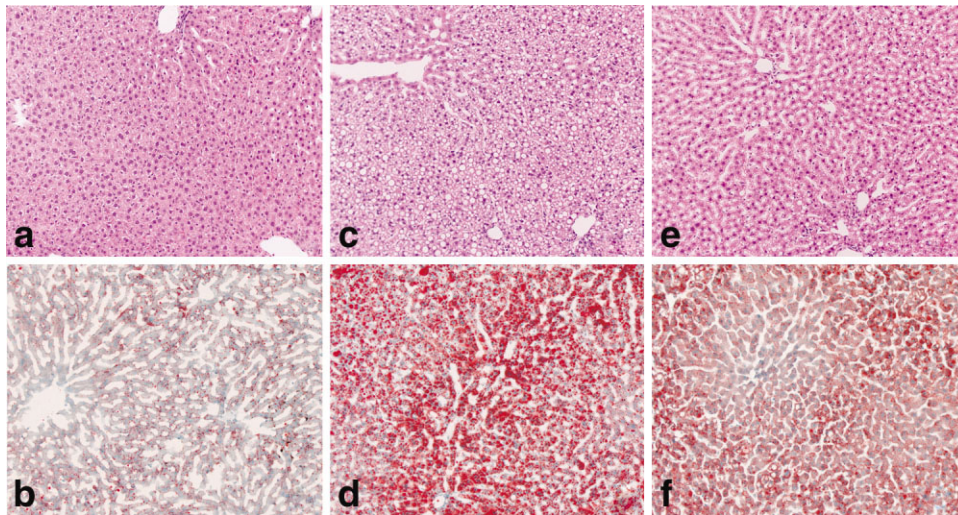


FIG. 3. Histological analyses of rat livers treated with vehicle and MTP inhibitor. Tissue sections were stained with H&E (top row) and oil red O (bottom row), which specifically stained the lipids. Note the strong lipid staining in (c and d) the 1-mg/kg dose animal, relatively less staining in (e and f) the 100-mg/kg dose animal, and no evidence of fatty liver in (a and b) the vehicle control animal (magnification = 10 \times).

from the in vivo study done at 2 T and the higher-resolution liver specimen study done at 7.1 T (Fig. 1). The resolution in the in vivo and specimen images was 0.089 mm³ and 0.0024 mm³, respectively, corresponding to a resolution increase of more than 100 \times and 4000 \times , respectively, relative to a typical clinical study. Subcutaneous fat and the 70% and 30% mineral oil phantoms are clearly highlighted in the fat image and suppressed in the water image. These provide a valuable internal control to the method. The higher resolution in the specimen images allowed us to define vascular anatomy and the lobular structure of the liver.

The hepatic signal intensities in the in-phase images (water images) were higher than those in the out-of-phase images (fat images) for all animal groups. No obvious focal differences in the fat images were seen between dose groups. Subtle increased intensities with dosed animals were only noted by more careful quantitative image analysis. Figure 2 summarizes the results of fat/water ratios measured on MRI and TG levels chemically quantitated with liver samples. The ratios of MR intensities for fat/water differed significantly between three groups in the dose-response study ($P < 0.01$). The means of fat/water ratios for the 1-mg/kg dose group animals were markedly increased to 20% \pm 5% compared to the control animals (5% \pm 0.6%; $P < 0.01$). The 100-mg/kg dose-treated animals showed a lower fat content (11% \pm 2%) (Fig. 2a) than the 1-mg/kg dose group, but a higher one than the control animals ($P < 0.01$). These results correlated well with the quantitative TG measurement of liver samples (Fig. 2b), and were confirmed visually in representative histologic sections (Fig. 3). Histology demonstrated normal hepatocytes in control rats, and centrilobular-to-panlobular intracellular fat vacuoles on MTP inhibitor-treated rats for both dose groups of 1 and 100 mg/kg. A slight-to-mild mononuclear cell infiltration was also appreciated. A strong lipid staining in the 1-mg/kg dose animals, and relatively less staining in the 100-mg/kg dose animals were clearly seen, with background evidence of lipid in vehicle control animals.

Serial comparisons of the fat/water ratio from the vehicle control animals in the three different groups of animals

revealed fat/water ratios of 4.9% \pm 0.5% through the entire course of the study for all three groups, indicating high reproducibility and biological variability for this quantitative technique in the longitudinal study (Fig. 4). The animals treated with MTP inhibitors showed a significant increase in the fatty component after 4 days of treatment ($P < 0.01$), and the highest fat/water ratio was observed after 14 days of treatment for all three study groups.

The specimen study was performed at the same time points as an additional validation of the in vivo studies. The absence of biological motion, operation at a higher field, and acquisition with a higher spatial resolution were expected to give a more accurate and reproducible measure of the fat/water changes. Figure 5 shows a linear time-dependent increased liver fatty component following the treatment with 1 mg/kg of MTP inhibitor from 10% \pm 4.3% to 57% \pm 15%, with a significant increase in liver fat fraction after 4 days of treatment ($P < 0.01$). The biological

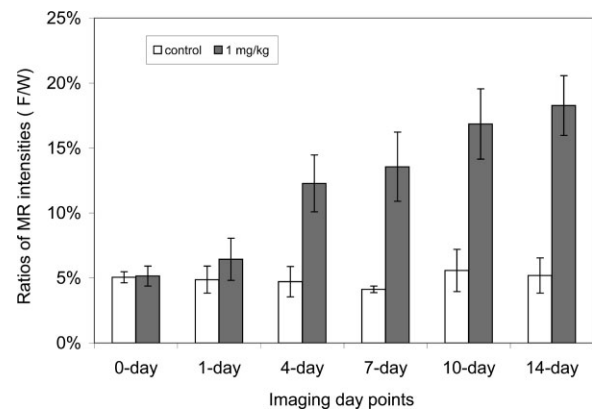


FIG. 4. Ratios of fat/water pooled from the three groups of animals at multiple points for the longitudinal study. The means of the fat/water ratios in these control animals throughout the study were 4.9% \pm 0.5%, suggesting a high level of consistency. A significant increase in the fatty component was noted after 4 days of treatment, and the highest fat/water ratio was observed after 14 days of treatment for all three study groups. The error bar indicates variation among the three groups (six animals).

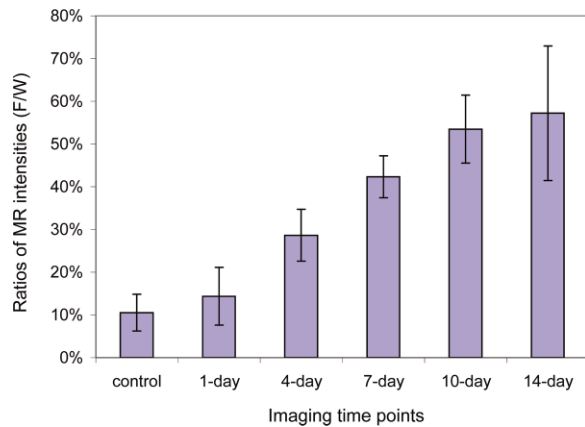


FIG. 5. Mean ratios of fat/water in the liver specimen study. Two slices per specimen and four ROIs per slice were selected from fat and water images. The error bar indicates variation among five animals. Note the significant increase in the liver fat fraction after 4 days of treatment with MTP inhibitor. [Color figure can be viewed in the online issue, which is available at www.interscience.wiley.com.]

response was very consistent, as shown by the small SD at each time point.

DISCUSSION

The liver is normally a non-adipose, highly cellular, solid organ tissue, and it has only a limited capacity for lipid storage. MTPs are located within the lumen of the endoplasmic reticulum of the hepatocyte, and are required for the secretion of lipoproteins. When an MTP inhibitor perturbs the system, the transfer of TG and cholesterol esters between liposomal membranes is diminished, resulting in dispersal of the triglycerides as small lipid droplets in the cytoplasmic matrix of hepatocytes (4,5,10). This histologic appearance is similar to the fatty infiltration produced nonspecifically by a variety of insults (e.g., the acute effects of alcohol, hepatitis, diabetes mellitus, obesity, and hepatotoxic drugs) (11). The quantification of the TG-filled droplets within the hepatocytes can be an important factor in assessing the status of lipid accumulation over time.

The potential of chemical-shift MRI for measuring the liver lipid content has long been appreciated, and several such techniques have been reported (12–15). To the best of our knowledge, the application of this technique for longitudinal monitoring of fatty liver at high resolution has not been reported previously. Extension of the 3D three-point Dixon method to small-animal imaging for this purpose is conceptually straightforward. However, significant technical challenges limit the accuracy of such measurements in small animals. The voxels required for small-animal imaging are >100 times smaller than those used in the clinical setting. It is critically important to control respiratory motion to achieve images of sufficient SNR to permit reproducible measurements. We addressed these challenges by developing a volume-encoding method and integrating scan-synchronous encoding with the sequence. The 3D encoding technique allows us to effectively average the signal over the entire volume of the liver. Scan-synchronous encoding was incorporated to eliminate

phase artifacts from respiratory motion. A triggered ventilating system allowed us to image the animals in vivo, in the absence of tissue hypoxia and respiratory motion. The respiratory motion was no longer problematic, and the levels of intrahepatic TG were consistent. The intrahepatic TG measured with other techniques may be low due to the exposure of animals to deep and prolonged anesthesia, which is likely a strong stimulus for intrahepatic lipolysis.

Although one might expect comparable increases of accumulated fat content in animals receiving similar doses, dissimilar fat/water ratios in animals dosed at the same levels were observed. This finding suggests that some pathological changes may be responsible for the different MR results in this study. An acute fatty liver form might have prolonged the T_1 and T_2 relaxation times due to changes in the plasma lipid levels and the subcellular ultrastructures, such as swelling and a mild decrease in the amount of mitochondria and disruption of the cristae, and vesicular transformation of the endoplasmic reticulum (17–19). These changes lead to an increase in the molar fraction of the free water and hence a decrease in the molar fraction of the bound water (19). Thus, intra- and extracellular alteration of hepatocytes in the T_1 and T_2 relaxation parameters may explain the contrary fat/water ratios in the same dosed animals. This hypothesis is supported by the specimen study, which showed the small SD of fat/water ratios in the same treatment point and three times higher fat/water ratios than that measured in the in vivo study for the 1-mg/kg dose groups. Many of the subcellular and pathological changes (e.g., cell swelling, plasma contents, and blood flow) that are responsible for the T_1 and T_2 relaxation parameters are not maintained when the specimen is immersed in formalin.

The image intensity in the in-phase and out-of-phase images is related to the fat content, and the fat and water relaxation times. One should consider the limitations of these techniques when applying the 3D three-point Dixon technique to the measurement of fat. First, in response to the MTP inhibitor treatment, the process of hepatocellular protein synthesis and excretion will be changed and the total plasma cholesterol levels will be decreased (1). Because the T_1/T_2 relaxation and magnetization transfer contrast of the tissue can be affected by the amount and mobility of indigenous tissue macromolecular contents, the quantitative data of the in vivo liver fat/water ratios should be viewed as relative, rather than absolute, values. Second, in biological tissues, there may be more variation in fat T_2 values, leading to a discrepancy between the detected and true fat contents. Although a short TE (5.4 ms) was selected, and it was assumed that the fat T_2 effects were negligible in this study, the fat image is the fraction of proton spins on fat molecules, which will differ from the fat fraction by weight because of the different densities of fat and water (16). Third, the specimen study did not reflect the gamut of tissue changes in all of the fatty livers, or the subcellular pathological changes. Thus, these techniques in combination with alternative methods using different mechanisms to differentiate the T_1 and T_2 relaxation times may be useful not only for quantitating the liver fat fraction, but also for determining the ultrastructural alteration of cytoplasmic organelles in hepatocytes (20).

CONCLUSIONS

We have demonstrated the quantitative application of the 3D three-point Dixon technique for longitudinal studies of fat in live rat liver. The method is highly reproducible and provides spatial information about distribution differences. With the increasing use of MRI for toxicologic studies, this method should provide an improved, noninvasive means of identifying and monitoring individuals with fatty liver.

ACKNOWLEDGMENTS

The authors thank Mr. Charles T. Wheeler and Dr. Lawrence W. Hedlund for their animal care, and Mr. Gary P. Cofer and Mr. William C. Kurylo for their support with the imaging. All MRI sessions were performed at the Duke Center for In Vivo Microscopy, an NIH/NCRR National Resource (P41 RR05959). Additional support provided by NCI (1 R24 CA92656) and Pfizer, Inc.

REFERENCES

- Dixon WT. Simple proton spectroscopy imaging. *Radiology* 1984;153:189–194.
- Glover GH. Multipoint Dixon technique for water and fat proton and susceptibility imaging. *J Magn Reson Imaging* 1991;1:521–530.
- Glover GH, Schneider E. Three-point Dixon technique for true water/fat decomposition with BO inhomogeneity correction. *Magn Reson Med* 1991;18:371–383.
- Wetterau JR, Gregg RE, Harrity TW, Arbeeny C, Cap M, Connolly G, Wetterau JR, Gregg RE, Harrity TW, Arbeeny C, Cap M, Connolly F, Chu CH, George RJ, Gordon DA, Jamil H, Jolibois KG, Kunselman LK, Lan SJ, Maccagnan TJ, Ricci B, Yan M, Young D, Chen Y, Fryszman OM, Logan JV, Musial CL, Poss MA, Robl JA, Simpkins LM, Biller SA, Slusarchyk WA, Sulsky R, Taunk P, Magnin DR, Tino JA, Lawrence RM, Dickson JK Jr., Biller SA. An MTP inhibitor that normalizes atherogenic lipoprotein levels in the WHHL rabbits. *Science* 1998;282:751–754.
- Robl JA, Sulsky R. A novel series of highly potent benzimidazole-based microsomal triglyceride transfer protein inhibitors. *J Med Chem* 2001;44:851–856.
- Hebbachi AM, Brown AM, Gibbons GF. Suppression of cytosolic triacylglycerol recruitment for very low density lipoprotein assembly by inactivation of microsomal triglyceride transfer protein results in a delayed removal of apoB-48 and apoB-100 from microsomal and Golgi membranes of primary rat hepatocytes. *J Lipid Res* 1999;40:1758–1768.
- Johnson GA, Hutchison JMS, Redpath W, Eastwood LM. Improvements in performance time for simultaneous three-dimensional NMR imaging. *J Magn Reson Imaging* 1983;54:374–384.
- Hedlund LW, Johnson GA. Mechanical ventilation for imaging the small animal lung. *ILAR J* 2002;43:159–174.
- Hurlston SE, Cofer GP, Johnson GA. Optimized receiver coils for increased SNR in MR microscopy. *Int J Imaging Syst Technol* 1997;8:277–284.
- Su GM, Sefton RM, Murray M. Down-regulation of rat hepatic microsomal cytochromes P-450 in microvesicular steatosis induced by orotic acid. *J Pharmacol Exp Ther* 1999;291:953–959.
- Caraceni P, Ryu HS, Subbotin V, De Maria N, Colantoni A, Roberts L, Trevisani F, Bernardi M, Van Thiel DH. Rat hepatocytes isolated from alcohol-induced fatty liver have an increased sensitivity to anoxic injury. *Hepatology* 1997;25:943–949.
- Lee JK, Dixon WT, Ling D, Levitt RG, Murphy Jr WA. Fatty infiltration of the liver: demonstration by proton spectroscopic imaging (preliminary observation). *Radiology* 1984;153:195–201.
- Fishbein MH, Garder KG, Potter CJ, Schmalbrock P, Smith MA. Introduction of fast MR imaging in the assessment of the hepatic steatosis. *Magn Reson Imaging* 1997;15:287–293.
- Levenson H, Greensite F, Hoefs J, Friloux L, Applegate L, Silva E, Kanel G, Buxton R. Fatty filtration of the liver: quantification with phase-contrast MR imaging at 1.5 T vs biopsy. *Am J Radiol* 1991;156:307–312.
- Fishbein MH, Stevens WR. Rapid MRI using a modified Dixon technique: a non-invasive and effective method for detection and monitoring of fatty metamorphosis of the liver. *Pediatr Radiol* 2000;31:806–809.
- Buxton RB, Wismer GL, Brady TJ, Rosen BR. Quantitative proton chemical-shift imaging. *Magn Reson Med* 1986;3:881–900.
- Stark DD, Bass NM, Moss AA, Bacon BR, McKerrow JH, Cann CE, Brito A, Goldberg HI. Nuclear magnetic resonance imaging of experimentally induced liver disease. *Radiology* 1983;148:743–751.
- Fantazzini P, Lendinara L, Novello F. Variation of the 1H spin-lattice relaxation in a fatty liver model as compared to normal liver. *Magn Reson Imaging* 1989;7:243–250.
- Chai JW, Lin YC, Chen JH, Wu CC, Lee CP, Chu WC, Lee SK. In vivo magnetic resonance (MR) study of fatty liver: importance of intracellular ultrastructural alteration for MR tissue parameters change. *J Magn Reson Imaging* 2000;14:35–41.
- Chen JH, Yeung HN, Lee SK, Chai JW. Evaluation of liver diseases via MTC and contrast agent. *J Magn Reson Imaging* 1999;2:257–265.